



**HAL**  
open science

## Jet noise prediction based on a self-adjoint operator

Etienne Spieser, Guillaume Bodard, Christophe Bailly

► **To cite this version:**

Etienne Spieser, Guillaume Bodard, Christophe Bailly. Jet noise prediction based on a self-adjoint operator. e-Forum Acusticum 2020, Dec 2020, Lyon, France. pp.1325-1332, 10.48465/fa.2020.0416 . hal-03221388

**HAL Id: hal-03221388**

**<https://hal.science/hal-03221388>**

Submitted on 21 May 2021

**HAL** is a multi-disciplinary open access archive for the deposit and dissemination of scientific research documents, whether they are published or not. The documents may come from teaching and research institutions in France or abroad, or from public or private research centers.

L'archive ouverte pluridisciplinaire **HAL**, est destinée au dépôt et à la diffusion de documents scientifiques de niveau recherche, publiés ou non, émanant des établissements d'enseignement et de recherche français ou étrangers, des laboratoires publics ou privés.

# JET NOISE PREDICTION BASED ON A SELF-ADJOINT OPERATOR

Étienne Spieser<sup>1,2</sup>

Guillaume Bodard<sup>1</sup>

Christophe Bailly<sup>2</sup>

<sup>1</sup> Safran Aircraft Engines, Rond Point René Ravaud - Réau, 77550 Moissy Cramayel, France

<sup>2</sup> École Centrale de Lyon, 36 avenue Guy de Collonge, 69131 Écully, France

etienne.spieser@ec-lyon.fr

## ABSTRACT

The adjoint method introduced by Tam and Auriault [1] enables the proper taking into account of acoustic propagation effects when jet noise is modelled from the statistics of a turbulent flow. This technique is recast in a systematic way valid for arbitrary propagation media, linear operators and sound sources. An acoustic analogy based on Pierce's wave equation for the acoustic potential [2] is proposed and Tam and Auriault's mixing noise model [3] is reformulated for this operator. This formulation presents three main advantages; no instability wave can occur since the acoustic energy conservation is enforced, then for being self-adjoint the adjoint solution to the propagation problem may straightforwardly be computed by flow reversal, finally Pierce's wave equation is a simple and cheap equation that several existing solver are able to solve. Work performed with *FFT*'s software *Actran TM* is presented illustrating the ability of a commercial tool to solve this equation and to compute adjoint Green's function required in statistical jet noise modelling.

## 1. INTRODUCTION

When jet noise predictions are based on an acoustic analogy, the source statistics are usually modelled from a RANS computation [3–5]. The propagation of sound to the observer is then achieved analytically using Green's function and a simplified flow model. This strategy is computationally less demanding than a direct noise computation, but often fails to correctly predict the acoustic propagation effects in complex configurations like those encountered for installed modern aircraft engines. With a smart use of the reciprocity principle, Tam and Auriault [1] introduced the adjoint method and enabled the tackling of propagation effects in complex environments, for which analytical Green's functions are unknown. In the aeroacoustic community adjoint Green's functions are usually sought as a solution to a scattering problem, and as such, are ill-posed to properly account for the surface refraction and edge diffraction phenomena. Yet in numerous applications, the effects of the latter are predominant [6]. The present contribution illustrates how the presence of surfaces can be dealt with in the computation of adjoint Green's functions with the commercial software *Actran TM*. RANS based mixing noise predictions are often conducted with Tam and

Auriault's model [3] that is detailed in the following section. The acoustic propagation equations considered by these authors are derived from the linearised Euler equations, and thus describe instability waves. Consequently, the method robustness is thereby regrettably deteriorated. This mixing noise model is recast here for the acoustic potential  $\phi$  as computed with Pierce's equation so as to achieve an acoustic preserving formulation. Moreover because *Actran TM* solves the wave equation of Möhring's acoustic analogy [7], a trick to solve Pierce's equation with this software is proposed. Finally, based on the flow reversal theorem (FRT), which proved to be equivalent to the adjoint approach for self-adjoint operators [8], an adjoint computation for a realistic aircraft engine is presented.

## 2. TAM AND AURIAULT'S MIXING NOISE MODEL

In a celebrated contribution, Tam *et al.* [9] gave experimental evidences for a separation in the mixing noise process of a jet foreseen by Ribner [10]. From this theory, two contributions arise in the noise caused by turbulent mixing; the first one is associated with the large-scales of the turbulence and second one finds its origin in the fine-scales. The mixing noise model of concern in this note is given by Tam and Auriault [3], and intends to model the sound radiated by the turbulence fine-scales. Since Lighthill's pioneer study [11], that lay out the basis for all acoustic analogies that would follow, it is admitted that jet mixing noise is driven by the unsteadiness of the Reynolds stress tensor. When the mean flow can be assumed to be incompressible this noise source term reads as  $\rho \mathbf{U} \otimes \mathbf{U} \approx \rho_0 \mathbf{U} \otimes \mathbf{U}$ , where  $\rho$ ,  $\mathbf{U}$  are the instantaneous density and velocity, and where  $\rho_0$  is the flow mean density [11, eq. (7)]. A Fourier filtering is considered by Tam and Auriault to remove the large-scales present in this sound source, and is noted in the following with an overbar. In their model, the noise source is then identified with the diagonal terms of the filtered Reynolds stress tensor  $\rho_0 \overline{\mathbf{U} \otimes \mathbf{U}}$ . These terms account for the fluid dilatation and compression. Based on the Boussinesq eddy viscosity model this source of sound can be directly related to the kinetic energy of the fine-scale turbulence per unit mass  $k_s$  with,  $\text{tr}(\rho_0 \overline{\mathbf{U} \otimes \mathbf{U}}) = 2\rho_0 k_s$ . An *isotropic* contribution of the modelled sound source  $q_s$  in the linearised momentum equation is then assumed, i.e. given in three dimensions by  $q_s = 2\rho_0 k_s/3$ , and

Lighthill's stress tensor is finally approximated in Tam and Auriault's model by,

$$\nabla \cdot (\rho_0 \overline{\mathbf{U} \otimes \mathbf{U}}) = \nabla q_s$$

Hence, the direct problem for Tam and Auriault's mixing noise writes,

$$\begin{cases} \rho_0 \frac{D(\mathbf{u})}{Dt} + \nabla p = -\nabla q_s \\ \frac{D(p)}{Dt} + \gamma p_0 (\nabla \cdot \mathbf{u}) = 0 \end{cases}$$

and can be recast by defining the associated linear operator  $\mathcal{L}_0$  into,

$$\mathcal{L}_0 \begin{pmatrix} \mathbf{u} \\ p \end{pmatrix} = \begin{pmatrix} -\nabla q_s \\ 0 \end{pmatrix}$$

where  $D/Dt = \partial/\partial t + \mathbf{u}_0 \cdot \nabla$  is the material derivative,  $\rho_0$ ,  $\mathbf{u}_0$ ,  $p_0$  are the mean flow fields and  $\mathbf{u}$ ,  $p$  the fluctuating ones. Note that the mean flow considered previously is parallel and that  $\mathcal{L}_0$  thus corresponds to the linearised Euler equations.

## 2.1 Governing adjoint equations

The governing adjoint equations are given by the Lagrange identity,

$$\left\langle \begin{pmatrix} \mathbf{u}^\dagger \\ p^\dagger \end{pmatrix}, \mathcal{L}_0 \begin{pmatrix} \mathbf{u} \\ p \end{pmatrix} \right\rangle = \left\langle \mathcal{L}_0^\dagger \begin{pmatrix} \mathbf{u}^\dagger \\ p^\dagger \end{pmatrix}, \begin{pmatrix} \mathbf{u} \\ p \end{pmatrix} \right\rangle$$

Accordingly to Tam and Auriault's model [3], the free-space propagation problem will be considered, for which all boundary conditions vanish for the direct problem as well as for the adjoint problem. In particular the radiating boundary conditions associated to the previously introduced direct problem and their associated anti-causal adjoint boundary conditions, will be discarded. Multiple integrations by parts, and taking benefit from the mean flow parallelism, subsequent adjoint operator  $\mathcal{L}_0^\dagger$  is obtained,

$$\begin{cases} -\rho_0 \frac{D(\mathbf{u}^\dagger)}{Dt} - \gamma p_0 \nabla p^\dagger = \mathbf{S}_{\rho_0 \mathbf{u}^\dagger}^\dagger \\ -\frac{D(p^\dagger)}{Dt} - \nabla \cdot \mathbf{u}^\dagger = S_{p^\dagger}^\dagger \end{cases}$$

where  $\mathbf{S}^\dagger = (S_{\rho_0 u_1^\dagger}^\dagger, S_{\rho_0 u_2^\dagger}^\dagger, S_{\rho_0 u_3^\dagger}^\dagger, S_{p^\dagger}^\dagger)^T$  is a generic writing of the adjoint source term. Because Tam and Auriault's model intends to compute the pressure field autocorrelation  $S_{pp}$  at a microphone position  $\mathbf{x}_m$ , a Dirac source term  $\delta_{\mathbf{x}_m, t_m} (\equiv \delta(\mathbf{x} - \mathbf{x}_m) \delta(t - t_m))$ , for mute space and time variables  $\mathbf{x}$  and  $t$  in the equation governing the adjoint field associated to the pressure  $p^\dagger$  is considered. Since an impulse response is considered, it follows that the corresponding adjoint fields  $\mathbf{u}^\dagger$  and  $p^\dagger$  are Green's functions. To bear in mind the source position  $\mathbf{x}_m$  and time  $t_m$ , this information will be specified in the notations of Green's functions, leading thus to the adjoint problem hereafter,

$$\mathcal{L}_0^\dagger \begin{pmatrix} \mathbf{u}_{\mathbf{x}_m, t_m}^\dagger \\ p_{\mathbf{x}_m, t_m}^\dagger \end{pmatrix} = \begin{pmatrix} \mathbf{0} \\ \delta_{\mathbf{x}_m, t_m} \end{pmatrix}$$

When replaced in Lagrange's identity together with the direct problem source term, the representation formula, analogue to [3, eq. (21)], is readily obtained,

$$\left\langle \begin{pmatrix} \mathbf{u}_{\mathbf{x}_m, t_m}^\dagger \\ p_{\mathbf{x}_m, t_m}^\dagger \end{pmatrix}, \begin{pmatrix} -\nabla q_s \\ 0 \end{pmatrix} \right\rangle = \left\langle \begin{pmatrix} \mathbf{0} \\ \delta_{\mathbf{x}_m, t_m} \end{pmatrix}, \begin{pmatrix} \mathbf{u} \\ p \end{pmatrix} \right\rangle$$

And finally with the property of the delta Dirac function,

$$p(\mathbf{x}_m, t_m) = - \left\langle \mathbf{u}_{\mathbf{x}_m, t_m}^\dagger, \nabla q_s \right\rangle$$

Following Tam and Auriault's steps, using integration by parts and the governing equation for  $p^\dagger$ , previous RHS is then reformulated as,

$$\begin{aligned} - \left\langle \mathbf{u}_{\mathbf{x}_m, t_m}^\dagger, \nabla q_s \right\rangle &= \left\langle \nabla \cdot \mathbf{u}_{\mathbf{x}_m, t_m}^\dagger, q_s \right\rangle \\ &= - \left\langle \frac{D(p_{\mathbf{x}_m, t_m}^\dagger)}{Dt}, q_s \right\rangle \\ &= \left\langle p_{\mathbf{x}_m, t_m}^\dagger, \frac{D(q_s)}{Dt} \right\rangle \end{aligned}$$

where again, all the contour integrals have been omitted since they vanish in free field. Note that  $\langle, \rangle$  has been used above indifferently for different size of vectors without ambiguity because the canonical scalar product is considered. This procedure can be applied for any scalar product, notice however that, as a step by step derivation would show, the latter needs to be adapted to each new couple of field considered.

## 2.2 Calculation of the pressure autocorrelation

Let the pressure  $p$  time-autocorrelation  $R_{pp}$  for a time-shift  $\tau$  at position  $\mathbf{x}_m$  be defined as,

$$R_{pp}(\mathbf{x}_m, \tau) = \int_{\mathbb{R}} dt_m p(\mathbf{x}_m, t_m) p(\mathbf{x}_m, t_m + \tau)$$

then Tam and Auriault's expression for the autocorrelation [3, eq. (24)] is retrieved:

$$R_{pp}(\mathbf{x}_m, \tau) = \int_{\mathbb{R}} dt_m \left\langle p_{\mathbf{x}_m, t_m}^\dagger, \frac{D(q_s)}{Dt} \right\rangle \left\langle p_{\mathbf{x}_m, t_m + \tau}^\dagger, \frac{D(q_s)}{Dt} \right\rangle$$

And the pressure time autocorrelation  $R_{pp}$ , simply expresses without assumptions,

$$R_{pp}(\mathbf{x}_m, \tau) = \int_{\Omega} d\mathbf{x}_1 \int_{\Omega} d\mathbf{x}_2 \int_{\mathbb{R}} dt_1 \int_{\mathbb{R}} dt_2 p_{\mathbf{x}_m}^\dagger(\mathbf{x}_1, t_1) p_{\mathbf{x}_m}^\dagger(\mathbf{x}_2, t_2 - \tau) R_{QQ}(\mathbf{x}_1, \mathbf{x}_2, \Delta t)$$

where  $\Delta t = t_1 - t_2$  and  $R_{QQ}(\mathbf{x}_1, \mathbf{x}_2, \Delta t)$  is the space-time autocorrelation of the quantity  $Q \equiv D(q_s)/Dt$ ,

$$R_{QQ}(\mathbf{x}_1, \mathbf{x}_2, \Delta t) = \int_{\mathbb{R}} dt_m \frac{D(q_s(\mathbf{x}_1, t_m + \Delta t))}{Dt_m} \frac{D(q_s(\mathbf{x}_2, t_m))}{Dt_m}$$

### 2.3 Modelling of the source autocorrelation term

The modelling of  $R_{QQ}$  cannot be further postponed, since its expression is needed to perform analytically the time integrations over  $dt_1$  and  $dt_2$ . The  $Q$ -quantity space-time autocorrelation model proposed by Tam and Auriault [3, eq. (27)] is shift-invariant, i.e. by defining  $\mathbf{r} = \mathbf{x}_1 - \mathbf{x}_2$ , then  $R_{QQ}(\mathbf{x}_1, \mathbf{x}_2, \Delta t) \equiv R_{QQ}(\mathbf{r}, \Delta t)$ , and writes,

$$R_{QQ}(\mathbf{r}, \Delta t) = \frac{\hat{q}_s^2}{c^2 \tau_s^2} \exp\left(-\frac{|\mathbf{r} \cdot \mathbf{u}_0|}{u_0^2 \tau_s} - \frac{\ln(2)}{l_s^2} (\mathbf{r} - \mathbf{u}_0 \Delta t)^2\right)$$

with  $u_0 = |\mathbf{u}_0|$ . The reader may refer to [3, §3] for the definition of the above other variables and their origin. In our applications the Fourier transformed pressure autocorrelation  $S_{pp}$  is of interest which is defined as,

$$S_{pp}(\mathbf{x}_m, \omega) = \int_{\mathbb{R}} d\tau R_{pp}(\mathbf{x}_m, \tau) e^{i\omega\tau}$$

where  $\alpha = \frac{l_s^2}{4 \ln(2) u_0^2}$  and  $\beta = \frac{\hat{q}_s^2 l_s}{c^2 \tau_s^2 u_0} \sqrt{\frac{\pi}{\ln(2)}}$ .

Fourier transforms are defined presently with,

$$F(\mathbf{x}, \omega) = \int_{\mathbb{R}} dt f(\mathbf{x}, t) e^{i\omega t}$$

and,

$$f(\mathbf{x}, t) = \frac{1}{2\pi} \int_{\mathbb{R}} d\omega F(\mathbf{x}, \omega) e^{-i\omega t}$$

Several change of variables, Fourier transforms, other integral manipulations, and defining  $\mathbf{r}_\perp = \mathbf{r} - (\mathbf{r} \cdot \mathbf{u}_0) \mathbf{u}_0 / u_0^2$ , lead to Tam and Auriault's equation (33) [3],

$$S_{pp}(\mathbf{x}_m, \omega) = \int_{\Omega} d\mathbf{x}_2 \int_{\Omega} d\mathbf{r} \beta p_{\mathbf{x}_m}^\dagger(\mathbf{r} + \mathbf{x}_2, \omega) p_{\mathbf{x}_m}^\dagger(\mathbf{x}_2, \omega)^* \exp\left(-\frac{|\mathbf{r} \cdot \mathbf{u}_0|}{u_0^2 \tau_s} - \frac{\ln(2)|\mathbf{r}_\perp|^2}{l_s^2} - i\omega \frac{\mathbf{r} \cdot \mathbf{u}_0}{u_0} - \alpha \omega^2\right)$$

### 2.4 Approximated calculation of the double space integration

The computation of the above double space integral is numerically unaffordable and a simplification is required.

#### 2.4.1 Fraunhofer approximation

Because in Tam and Auriault's work the observer is set in the acoustic far field, those authors proposed to model two neighbour acoustic ray paths from the source region by a Fraunhofer-like approximation [3, fig. 4, eq. (34)], which expresses with vector notations as,

$$p_{\mathbf{x}_m}^\dagger(\mathbf{r} + \mathbf{x}_2, \omega) \approx p_{\mathbf{x}_m}^\dagger(\mathbf{x}_2, \omega) \exp\left(\frac{i\omega \mathbf{x}_m \cdot \mathbf{r}}{a_\infty |\mathbf{x}_m|}\right)$$

where  $a_\infty$  is the ambient speed of sound. Note that this expression differs from the one proposed in the literature by the phase shift sign [3]. By defining  $\mathbf{x}_{m,\perp} = \mathbf{x}_m - (\mathbf{x}_m \cdot \mathbf{u}_0) \mathbf{u}_0 / u_0^2$ , and replacing this formula in the expression of

$S_{pp}$ , the double integral simplifies into,

$$S_{pp}(\mathbf{x}_m, \omega) = \int_{\Omega} d\mathbf{x}_2 \frac{2\hat{q}_s^2 l_s^3}{c^2 \tau_s} \left(\frac{\pi}{\ln(2)}\right)^{3/2} \left| p_{\mathbf{x}_m}^\dagger(\mathbf{x}_2, \omega) \right|^2 \frac{\exp\left(\frac{-\omega^2 l_s^2}{4 \ln(2) u_0^2} \left(1 + \frac{u_0^2 |\mathbf{x}_{m,\perp}|^2}{a_\infty^2 |\mathbf{x}_m|^2}\right)\right)}{1 + \omega^2 \tau_s^2 \left(1 - \frac{\mathbf{u}_0 \cdot \mathbf{x}_m}{a_\infty |\mathbf{x}_m|}\right)^2}$$

which is Tam and Auriault's fine-scale mixing noise formula [3, eq. (35)]. Note that above expression differs from the original one by a factor of  $2\pi$ , which is related to different Green's function definition, refer to [3, eq. (19)], from which a  $4\pi^2$  factor appears; then because of differences in the Fourier transform conventions, see [3, eq. (25)], the present relation should be divided by  $2\pi$  to comply with Tam and Auriault's relation. Note furthermore that the here presented expression is slightly enhanced compared to the original one, since it can tackle three dimensional propagation problems.

#### 2.4.2 Taylor expansion

As suggested by Lielens [12], if adjoint Green's function  $p_{\mathbf{x}_m}^\dagger$  is computed numerically for a near-field propagation problem, the knowledge of its spatial evolution can be capitalised and the Fraunhofer approximation can be replaced by a Taylor expansion; this paragraph presents the corresponding formula. If  $\mathbf{r} = \mathbf{x}_1 - \mathbf{x}_2$  is small  $p_{\mathbf{x}_m}^\dagger(\mathbf{r} + \mathbf{x}_2, \omega)$  can be approximated by the first order Taylor expansion,

$$p_{\mathbf{x}_m}^\dagger(\mathbf{r} + \mathbf{x}_2, \omega) \approx p_{\mathbf{x}_m}^\dagger(\mathbf{x}_2, \omega) + \mathbf{r} \cdot \frac{\partial p_{\mathbf{x}_m}^\dagger(\mathbf{x}_2, \omega)}{\partial \mathbf{x}_2}$$

Replacing this expression in the formula for  $S_{pp}$  leads to following expression for the pressure autocorrelation,

$$S_{pp}(\mathbf{x}_m, \omega) = \int_{\Omega} d\mathbf{x}_2 \frac{2\hat{q}_s^2 l_s^3}{c^2 \tau_s} \left(\frac{\pi}{\ln(2)}\right)^{3/2} p_{\mathbf{x}_m}^\dagger(\mathbf{x}_2, \omega)^* \frac{\exp\left(-\frac{\omega^2 l_s^2}{4 \ln(2) u_0^2}\right)}{1 + \omega^2 \tau_s^2} \left( p_{\mathbf{x}_m}^\dagger(\mathbf{x}_2, \omega) - \frac{2i\omega \tau_s^2}{1 + \omega^2 \tau_s^2} \left( \mathbf{u}_0 \cdot \frac{\partial p_{\mathbf{x}_m}^\dagger(\mathbf{x}_2, \omega)}{\partial \mathbf{x}_2} \right) \right)$$

### 3. TAM AND AURIAULT'S FORMULA APPLIED TO PIERCE'S WAVE EQUATION

Tam and Auriault's formula [3, eq. (35)] relies on the prior computation of adjoint Green's function  $p_{\mathbf{x}_m}^\dagger$  recalled by the above set of equations. This presents two limitations for the practical use of this theory; firstly efficient solvers that can twofold compute these equations and handle complex geometries are scarce, and secondly as for the direct problem, these equations do also present physical unstable modes. A reformulation of Tam and Auriault's formula with a propagation operator based on Pierce's equation [2, eq. (27)] is a way of overcoming these difficulties. The formulation proposed by Pierce based on the acoustic potential  $\phi$  is indeed energy preserving and solvers, e.g.

Actran TM from FFT can be configured to solve this wave equation.

The acoustic analogy based on Pierce's wave equation writes,

$$\frac{D^2(\phi)}{Dt^2} - \nabla \cdot (a_0^2 \nabla \phi) = \frac{D(S_m)}{Dt} - S_p$$

and,

$$\Delta S_m = \nabla \cdot (\rho_0 \mathbf{S}_u)$$

where  $(\mathbf{S}_u, S_p)$  is the general writing of a source term for the linearised momentum and energy equations. Because Pierce's wave equation describes solely the propagation of potential acoustic fluctuations  $\phi$ , the source term for this equation needs to be potential as well. This is the meaning of the introduction of the linearised momentum source potential  $S_m$ . From the source model for mixing noise of Tam and Auriault's, it comes directly that  $S_m = -q_s$  and  $S_p = 0$ . The pressure field  $p$  is then rebuilt subsequently from the acoustic potential  $\phi$  considering  $p = -D(\phi)/Dt$  while the fluctuating velocity field is computed with  $\rho_0 \mathbf{u} = \nabla \phi$ .

### 3.1 Pressure autocorrelation with an acoustic potential description

Pierce's wave equation is self-adjoint for the canonical scalar product, and its adjoint Green's function is defined by,

$$\frac{D^2(\phi_{\mathbf{x}_m, t_m}^\dagger)}{Dt^2} - \nabla \cdot (a_0^2 \nabla \phi_{\mathbf{x}_m, t_m}^\dagger) = \delta_{\mathbf{x}_m, t_m}$$

The application of Lagrange's identity then gives,

$$\phi(\mathbf{x}_m, t_m) = \langle \phi_{\mathbf{x}_m, t_m}^\dagger, -\frac{D(q_s)}{Dt} \rangle$$

The pressure time autocorrelation is hence defined by,

$$\begin{aligned} R_{pp}(\mathbf{x}_m, \tau) &= \int_{\mathbb{R}} dt_m p(\mathbf{x}_m, t_m) p(\mathbf{x}_m, t_m + \tau) \\ &= \int_{\mathbb{R}} dt_m \frac{D(\phi)}{Dt_m, \mathbf{x}_m} \frac{D(\phi)}{Dt_m + \tau, \mathbf{x}_m} \end{aligned}$$

where  $D/D_{t_i, \mathbf{x}_j} = \partial/\partial t_i + \mathbf{u}_0 \cdot \partial/\partial \mathbf{x}_j$  is the material derivative with respect to  $\mathbf{x}_j$  and the reference time  $t_i$ .

### 3.2 Far-field prediction formula with wind

After some algebra very similar to those performed by Tam and Auriault [3], and with the same source model, the prediction formula expresses in the far-field, i.e. owing on a Fraunhofer approximation, as,

$$\begin{aligned} S_{pp}(\mathbf{x}_m, \omega) &= \int_{\Omega} d\mathbf{x}_2 \frac{2\hat{q}_s^2 l_s^3}{c^2 \tau_s} \left( \frac{\pi}{\ln(2)} \right)^{3/2} \\ &\left| D_{-\mathbf{u}_0, \mathbf{x}_m} \left( \phi_{\mathbf{x}_m}^\dagger(\mathbf{x}_2, \omega) \right) \right|^2 \frac{\exp \left( \frac{-\omega^2 l_s^2}{4 \ln(2) u_0^2} \left( 1 + \frac{u_0^2 |\mathbf{x}_{m, \perp}|^2}{a_\infty^2 |\mathbf{x}_m|^2} \right) \right)}{1 + \omega^2 \tau_s^2 \left( 1 - \frac{\mathbf{u}_0 \cdot \mathbf{x}_m}{a_\infty |\mathbf{x}_m|} \right)^2} \end{aligned}$$

where  $D_{-\mathbf{u}_0, \mathbf{x}_m} = -i\omega - \mathbf{u}_0 \cdot \partial/\partial \mathbf{x}_m$  is the material derivative at the observer location written in the frequency domain with reversed flow. For a far-field observer  $\mathbf{x}_m$  and with a constant free-stream wind as depicted in figure 1, the expression of this material derivative can be computed analytically. Recall that the adjoint field  $\phi_{\mathbf{x}_m}^\dagger$  is

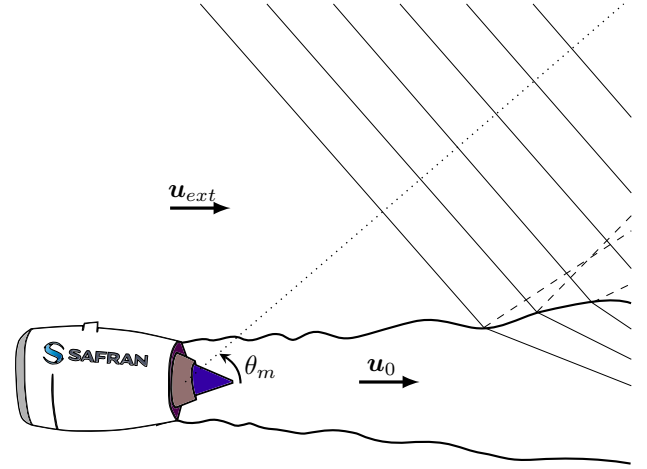


**Figure 1.** When the microphone is in the acoustic far field, the polar angle  $\theta_m$  is enough to characterise the adjoint function of a round jet.

anti-causal and travels outward of the domain. Neglecting the azimuthal dependence, the mixing noise prediction formula in presence of wind writes,

$$\begin{aligned} S_{pp}(\theta_m, \omega) &= \int_{\Omega} d\mathbf{x}_2 \frac{2\omega^2 \hat{q}_s^2 l_s^3}{c^2 \tau_s} \left( \frac{\pi}{\ln(2)} \right)^{3/2} \left| \phi_{\theta_m}^\dagger(\mathbf{x}_2, \omega) \right|^2 \\ &\left( 1 + \frac{M_{ext} \cos \theta_m}{1 + M_{ext} \cos \theta_m} \right)^2 \frac{\exp \left( \frac{-\omega^2 l_s^2}{4 \ln(2) u_0^2} (1 + M_\infty^2 \sin^2 \theta_m) \right)}{1 + \omega^2 \tau_s^2 (1 - M_\infty \cos \theta_m)^2} \end{aligned}$$

where  $M_\infty = |\mathbf{u}_0|/a_\infty$  and  $M_{ext} = |\mathbf{u}_{ext}|/a_\infty$  and with the adjoint source, i.e. the microphone, set in the far-field, that is  $\phi_{\mathbf{x}_m}^\dagger(\mathbf{x}_2, \omega) \rightarrow \phi_{\theta_m}^\dagger(\mathbf{x}_2, \omega)$ , where  $\theta_m$  is the jet polar angle as defined in figure 1.

## 4. COMPUTING ADJOINT GREEN'S FUNCTION $\phi_{\mathbf{x}_m}^\dagger$ WITH ACTRAN TM

A recent investigation by the authors has shown that adjoint solutions to propagation problems could be computed equivalently for self-adjoint operators with the so called flow reversal theorem (FRT) [8]. The FRT states that the reciprocal acoustic solution over a moving flow can be obtained by simply reversing the direction of the flow. A procedure for this applied for Pierce's equation is presented here with FFT's commercial software, *Actran TM*.

### 4.1 Equation solved in *Actran TM*

*Actran TM* is a finite element code written in the frequency domain capable of handling complex geometries. This

software solves Mörhing's equation written for the normalised fluctuating stagnation enthalpy  $b$ ,

$$\frac{\partial}{\partial t} \left[ \frac{\rho_0}{\rho_{T,0}^2 a_0^2} \frac{Db}{Dt} \right] + \nabla \cdot \left[ \frac{\rho_0 \mathbf{u}_0}{\rho_{T,0}^2 a_0^2} \frac{Db}{Dt} - \frac{\rho_0}{\rho_{T,0}^2} \nabla b \right] = S$$

*Actran TM* solves in the frequency domain, some generic monopole  $S_m$  and dipole  $S_d$  source definition [13],

$$S = \frac{\partial S_m}{\partial t} + \nabla \cdot S_d$$

By introducing the Mach number  $M_0 = \mathbf{u}_0/a_0$ , the mean total density  $\rho_{T,0}$  is given by,

$$\rho_{T,0} = \rho_0 \left( 1 + \frac{\gamma-1}{2} M_0^2 \right)^{1/(\gamma-1)}$$

The pressure is built then subsequently with,

$$\frac{\rho_{T,0}}{\rho_0} \frac{\partial p}{\partial t} = \frac{Db}{Dt}$$

Note that this equation is linear while the equation given by Mörhing [7] for the stagnation enthalpy  $B$  is not. The latter is rescaled accordingly with,

$$\delta b = \rho_{T,0} \delta B$$

## 4.2 Solving Pierce's equation with *Actran TM*

In *FFT's* software, it is not possible however to force the equality  $\rho_{T,0} = \rho_0$ , so as to solve Pierce's equation. This is because the expression of the mean stagnation density  $\rho_{T,0}$  is directly computed from the mean density  $\rho_0$  and the mean Mach number  $M_0$ . This hardship is overcome by preprocessing the mean flow fields  $\rho_0$ ,  $p_0$  and  $\mathbf{u}_0$  given in input, so to compensate in the solved equation the presence of the total mean density  $\rho_{T,0}$ . The source amplitude needs to be corrected along with this transformation.

### 4.2.1 Preprocessing of the mean flow given in input

A similar manipulation was performed by Legendre [13] to rebuild Mörhing's equation with *Actran TM* without the  $\rho_{T,0}$  normalisation. Some customised mean flow fields are defined here in order for *Actran TM* to solve Pierce's equation for the physically relevant mean flow fields  $\rho_0$ ,  $p_0$  and  $\mathbf{u}_0$ . Let these customised variables be renamed by adding a  $C$  in subscript. An inspection of *Actran TM's* equation and Pierce's one indicates that subsequent transformations need to be achieved,

$$\mathbf{u}_{0,C} \leftarrow \mathbf{u}_0 \quad a_{0,C} \leftarrow a_0 \quad \frac{\rho_{0,C}}{\rho_{T,0}^2} \leftarrow \frac{1}{\rho_0}$$

where this time,

$$\rho_{T,0} = \rho_{0,C} \left( 1 + \frac{\gamma-1}{2} \frac{\rho_{0,C}}{\gamma p_{0,C}} \mathbf{u}_{0,C}^2 \right)^{1/(\gamma-1)}$$

It comes out, that the mean velocities  $\mathbf{u}_0$  and  $a_0$  are not affected by these transformations. Therefore, because the

mean density  $\rho_0$  is modified, the mean pressure  $p_0$  needs to be corrected in order for  $a_0 = \sqrt{\gamma p_0/\rho_0}$  to remain unchanged. Finally, to solve Pierce's equation with *Actran TM*, the adjustment that should be applied to the mean flow field to obtain the suitable corrected input fields  $\rho_{0,C}$  and  $p_{0,C}$  reads,

$$\frac{p_{0,C}}{p_0} = \frac{\rho_{0,C}}{\rho_0} = \left[ 1 + \frac{\gamma-1}{2} \frac{\mathbf{u}_0^2}{a_0^2} \right]^{-2/(\gamma-1)}$$

### 4.2.2 Correction of the source amplitude

In *Actran TM*, there are three kinds of source amplitude definitions, sources referred to as 'P' type, 'Q' type or 'V' type (cf. keyword 'AMPLITUDE\_TYPE'). The type 'P' amplitude is default and is related to the pressure field, while the 'Q' type amplitude is related to the mass flow rate and the 'V' type source is related to the volume source. In the present study, a source amplitude of type 'P' is considered. When the above preprocessing step is conducted to turn *Actran TM* into a Pierce's equation solver, the acoustic potential  $\phi$  solution of Pierce's normalised equation, given for  $\delta_{\mathbf{x}_s}$  a pointwise source in  $\mathbf{x}_s$  by,

$$\frac{1}{a_0^2} \left( \frac{D^2 \phi}{Dt^2} - \nabla \cdot (a_0^2 \nabla \phi) \right) = A \delta_{\mathbf{x}_s}$$

is related to the computed stagnation enthalpy  $b$  by,

$$\phi^* = \frac{-i\omega A}{4} \left( 1 + \frac{\gamma-1}{2} M_{0,S}^2 \right)^{-1/(\gamma-1)} b$$

where  $\phi^*$  is the complex conjugate of  $\phi$ ,  $A$  the complex source amplitude defined in the software,  $\omega$  the investigated acoustic pulsation and  $M_{0,S}$  the Mach number at the source position. This amplitude correction depends only on  $a_0$  and  $M_0$  and is therefore insensitive to the  $\rho_{0,T}$  correction procedure.

## 4.3 Validation of *Actran TM's* hijacking

The proposed reconstruction procedure of Pierce's equation with *Actran TM* is validated for a uniform mean flow. For the bidimensionnal problem of a monopole set in an uniform mean flow the solution is known analytically. Figure 2 presents  $\phi$  for a pointwise source set at the origin, where  $\omega = 20\pi \text{ rad.s}^{-1}$ ,  $M_0 = 0.756$ ,  $p_0 = 103330 \text{ Pa}$ ,  $T_0 = 300 \text{ K}$  and  $a_0 = \sqrt{\gamma R T_0}$ . An almost perfect match presented in figure 3 is obtained for this simple flow model.

## 4.4 Illustrative computation for a realistic engine

Having recourse to a commercial software like *Actran TM* for the computation of adjoint solutions is attractive because such a tool is versatile and robust. Capabilities of *Actran TM* to compute adjoint solutions for jet noise relevant configurations is illustrated here. *Actran TM* enables amongst others the reading of RANS computations, the generation and the handling of unstructured meshes, the interpolation of the flow on the acoustic grid, the computation and the post-processing of the results. For the purpose

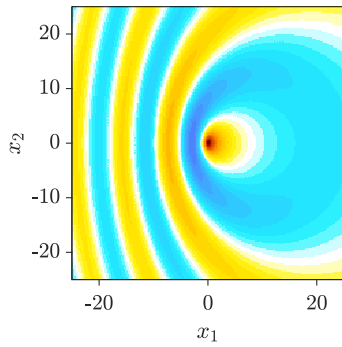


**Figure 2.** Acoustic potential field  $\phi$  for the considered uniform mean flow.

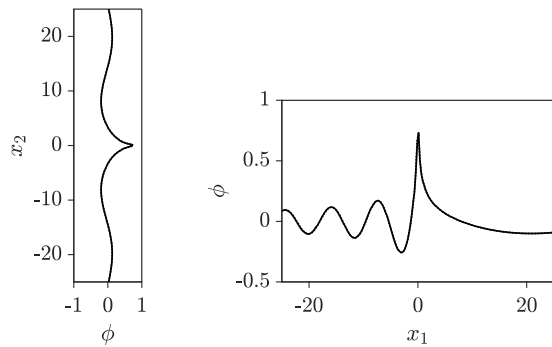


**Figure 3.** Extracts along  $x_1 = 0$  and  $x_2 = 0$  of the acoustic potential field  $\phi$  computed with *Actran TM* — and the analytical solution .....

of illustrating the methodology execution, the EXEJET dual-stream engine with chevrons is considered here [14]. The dealt configuration presents realistic features of an aircraft engine. The primary jet exiting the core is heated with respect to the secondary flow originating from the fan with a temperature ratio  $T_c/T_f \approx 2.6$ . The local jet Mach numbers for both flow are respectively  $M_f = 0.84$  and  $M_c = 0.67$ . Some in-flight effects are moreover accounted for with an external flow of  $M_{ext} = 0.27$ . The geometry presents 9 inner chevrons and 18 outer chevrons, so that the flow simulation could benefit from angular periodicity simplifications, and hence only an angular sector of  $20^\circ$  of the flow was modelled with RANS. In order to rebuild the complete engine, an intermediate grid of  $40^\circ$  angle is first created. The *Boxpro* toolbox of *ActranVI* enables to duplicate the  $20^\circ$  geometry and to generate an unstructured mesh such as presented in figure 4 (use *interior shrinkwrap* for multi-bloc geometries). An unstructured acoustic mesh of 3.9 million three-dimensional linear elements (800 000 nodes) is generated for a cylindrical domain presenting a diameter of 3 engine diameters and a length of 10 diameters. The mean flows are imported from a RANS computation and interpolated over the acoustic mesh as presented in figure 5. This figure also depicts the reversed mean flow required for the execution of the flow reversal theorem. This enables the computation of the adjoint solution to Pierce's equation.

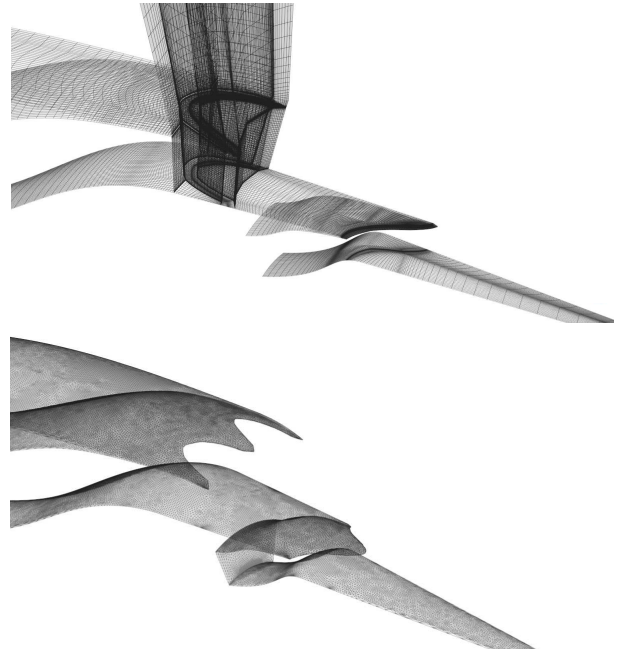


**Figure 4.** Detail of the structured and multi-bloc CFD mesh spanning on  $20^\circ$  used for the RANS computation (top) and detail of the unstructured acoustic mesh computed with planar symmetry used to rebuilt the full  $360^\circ$  flow field thanks to the geometry periodicity (bottom).

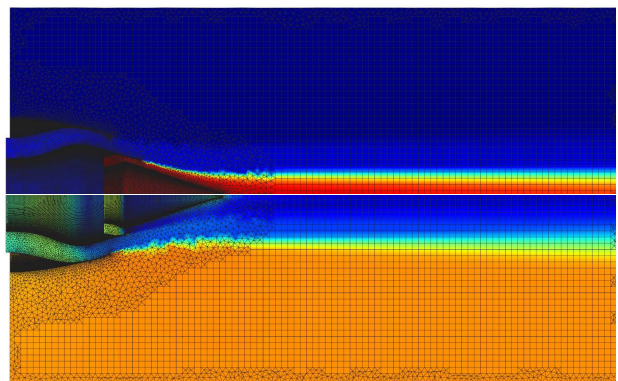


**Figure 5.** Mean speed of sound  $a_0$  from  $331\text{m.s}^{-1}$  to  $570\text{m.s}^{-1}$  (top) and mean axial velocity  $u_{0,1}$  from  $-377\text{m.s}^{-1}$  to  $3.37\text{m.s}^{-1}$  (bottom) interpolated on the generated acoustic mesh.

Figure 6 presents the acoustic potential computed over the reversed mean flow for a compact source oscillating at a Strouhal number of  $St_f = 2.0$ . Where  $St_f = \frac{1}{M_f} \frac{D_f}{\lambda}$  is based on the fan flow exit diameter  $D_f$ . This corresponds to a mixed Strouhal number [14] of  $St_{mix} = 1.3$ . Computations performed for adjoint sources set in the near-field, and for a source exterior to the computation domain. The acoustic field computed thereby, is sought adjoint Green's function  $\phi^\dagger$ . For this configuration 85 GB of RAM and about 45min per frequency were required with a sequential use of the MUMPS solver. Reminding from Lagrange's identity that the adjoint field  $\phi^\dagger$  is relevant where the physical sound source are located, commentaries on the adjoint

fields must focus on the jet sheared flow region. It is seen in figure 6 that the adjoint solution presents some sharp variations in phase in these regions. This may translate into constructive and destructive interferences in the radiated field. It is expected that reliable computations of adjoint Green's solutions notably improve the taking into account of acoustic propagation effects. In future work, attention will be paid in a step by step validation of the complete jet mixing noise prediction methodology. In particular, it appears instructive to compare the original Tam and Auriault mixing noise model [3] using parallel flow analytical adjoint Green's functions [15] to the more general alternative proposed in the present work. Whenever installation effects are present, it is expected that the proposed formulation offers a significant amelioration in the acoustic predictions.

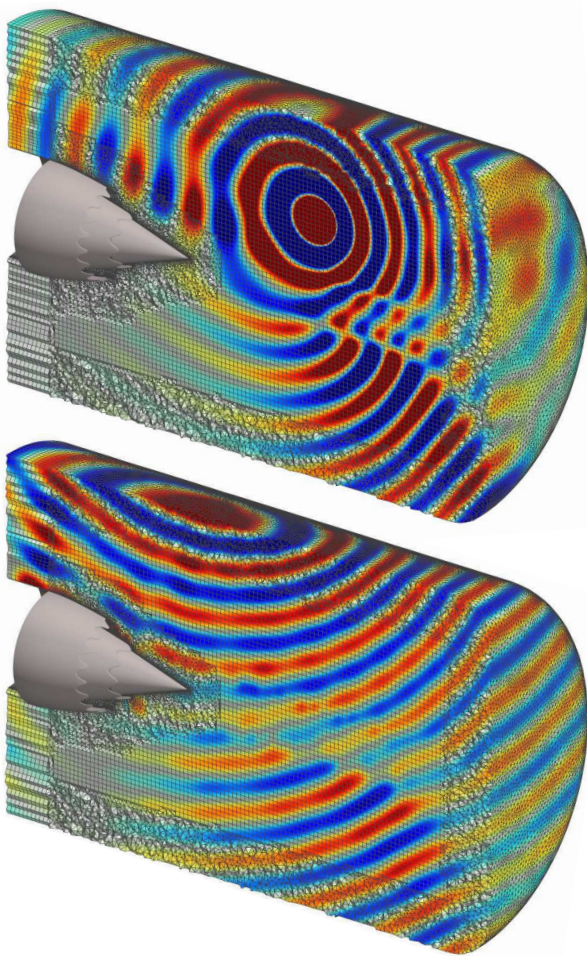


**Figure 6.** Adjoint Green's function  $\phi^\dagger$  of Pierce's equation computed with the flow reversal theorem for  $St_f = 2.0$ . The near-field solutions to the reciprocal propagation problem exhibits a complex behaviour in the jet flow region (top). The computations for a source exterior to the computation domain at a distance of  $10D_f$  from the engine is presented (bottom).

## 5. CONCLUSION

In this contribution the mixing noise model of Tam and Auriault [3] is recalled and recast for Pierce's wave equation which is twofold stable and self-adjoint. Because this potential acoustic wave equation is self-adjoint, its adjoint solution can be computed with the flow reversal theorem (FRT). A procedure to transform the equation solved by *Actran TM* into Pierce's equation is used and validated for an uniform mean flow. Eventually the illustrative computation of adjoint solutions for a aircraft engine with flight effects is presented. A realistic turbofan engine geometry with chevrons is considered as a proof of concept and different adjoint fields are computed in near and far field to a reasonable computational cost ( $St = 2$ , 45 min per frequency, 85 GB of RAM). The source does not need to be meshed and can be set exterior to the computational domain in *Actran TM*. These results are all the more encouraging, as no special effort was made to minimise the computational costs (mesh optimisation, use of parallel solver). A significant asset of the formulation, as presented here, is its ability to account for the presence of surfaces in the acoustic propagation problem. Future work will have to focus on implementing the entire prediction chain, from the calculation of the RANS solution to the noise spectrum, and to validate each step.

## 6. ACKNOWLEDGEMENT

The authors would like to acknowledge C. Legendre and the *FFT* team for their support and fruitful discussions. The first author is funded by Safran Aircraft Engines (CIFRE 2017/0229), with also the support of the Labex CeLyA of the Université de Lyon, within the programme "Investissements d'Avenir" (ANR-10-LABX-0060/ANR-11-IDEX-0007) operated by the French National Research Agency (ANR).

## 7. REFERENCES

- [1] C. K. W. Tam and L. Auriault, "Mean flow refraction effects on sound radiated from localized source in a jet," *Journal of Fluid Mechanics*, vol. 370, pp. 149–174, 1998.
- [2] A. D. Pierce, "Wave equation for sound in fluids with unsteady inhomogeneous flow," *The Journal of the Acoustical Society of America*, vol. 87, no. 6, pp. 2292–2299, 1990.
- [3] C. K. W. Tam and L. Auriault, "Jet mixing noise from fine-scale turbulence," *AIAA Journal*, vol. 37, no. 2, pp. 145–153, 1999.
- [4] W. Béchara, P. Lafon, C. Bailly, and S. M. Candel, "Application of a  $\kappa$ - $\varepsilon$  turbulence model to the prediction of noise for simple and coaxial free jets," *The Journal of the Acoustical Society of America*, vol. 97, no. 6, pp. 3518–3531, 1995.

- [5] P. J. Morris and S. A. E. Miller, “Prediction of broadband shock-associated noise using reynolds-averaged navier-stokes computational fluid dynamics,” *AIAA Journal*, vol. 48, no. 12, pp. 2931–2944, 2010.
- [6] A. Mosson, D. Binet, and J. Caprile, “Simulation of the installation effects of the aircraft engine rear fan noise with ACTRAN/DGM,” in *20th AIAA/CEAS Aeroacoustics Conference*, (Atlanta, Georgia), AIAA Paper 2014-3188, 2014.
- [7] W. Möhring, “A well posed acoustic analogy based on a moving acoustic medium,” in *Aeroacoustic workshop SWING*, (Dresden), 1999.
- [8] É. Spieser and C. Bailly, “Sound propagation using an adjoint-based method,” *Journal of Fluid Mechanics*, vol. 900, p. A5, 2020.
- [9] C. K. W. Tam, M. Golebiowski, and J. Seiner, “On the two components of turbulent mixing noise from supersonic jets,” in *2nd AIAA/CEAS Aeroacoustics Conference*, (State College, Pennsylvania), AIAA Paper 1996-1716, 1996.
- [10] H. S. Ribner, “Quadrupole correlations governing the pattern of jet noise,” *Journal of Fluid Mechanics*, vol. 38, no. 1, pp. 1–24, 1969.
- [11] M. J. Lighthill, “On sound generated aerodynamically I. General theory,” in *Proceedings of the Royal Society of London. Series A. Mathematical and Physical Sciences*, vol. 1107, pp. 564–587, The Royal Society London, 1952.
- [12] G. Lielens. Free Field Technologies, personal communication, Mont-Saint-Guibert, 11/09/2019.
- [13] C. Legendre. Free Field Technologies, communication via e-mail, 17/07/2019.
- [14] J. Huber, C. Drochon, A. Pintado-Peno, F. Cléro, and G. Bodard, “Large-scale jet noise testing, reduction and methods validation “EXEJET”: 1. project overview and focus on installation,” in *20th AIAA/CEAS Aeroacoustics Conference*, (Atlanta, Georgia), AIAA Paper 2014-3032, 2014.
- [15] M. Z. Afsar, A. Sescu, V. Sassanis, and S. K. Lele, “Supersonic jet noise predictions using a unified asymptotic approximation for the adjoint vector Green’s function and LES data,” in *23rd AIAA/CEAS Aeroacoustics Conference*, (Denver, Colorado), AIAA Paper 2017-3030, 2017.